

Article

Innovative Methods for Intensifying the Processing of Zinc Clinker: Synergy of Microwave Treatment and Ultrasonic Leaching

Bagdaulet Kenzhaliyev, Tatiana Surkova, Ainur Berkinbayeva , Zhazira Baltabekova, Kenzhegali Smailov *, Yerkezhan Abikak, Shynar Saulebekkyzy , Nazerke Tolegenova, Tursynkul Omirbek * and Zamzagul Dosymbaeva

The Institute of Metallurgy and Ore Beneficiation, Satbayev University, Almaty 050013, Kazakhstan; bagdaulet_k@satbayev.university (B.K.); t.surkova@satbayev.university (T.S.); a.n.berkinbayeva@satbayev.university (A.B.); zh.baltabekova@satbayev.university (Z.B.); a.abikak@satbayev.university (Y.A.); sh.saulebekkyzy@satbayev.university (S.S.); 000219600614-m@stud.satbayev.university (N.T.); z.dossymbayeva@satbayev.university (Z.D.)

* Correspondence: k.smailov@satbayev.university (K.S.); 971202400632-m@stud.satbayev.university (T.O.); Tel.: +7-747-6536293 (K.S.); +7-747-6287095 (T.O.)

Abstract: This study presents an innovative approach to processing refractory zinc-bearing clinker through the synergistic application of microwave thermal treatment and ultrasonic-assisted leaching. Microwave irradiation induces phase transformations in the clinker, improving its reactivity and facilitating subsequent zinc dissolution, while ultrasonic cavitation enhances mass transfer by disrupting passivation layers. Key process parameters, including acid concentration, temperature, pulp density, and leaching time, were systematically investigated using response surface methodology (RSM) and central composite design (CCD). The results demonstrate that the optimized process conditions led to a significant increase in zinc recovery from refractory materials.



Academic Editors: Corby G. Anderson and Petros E. Tsakiridis
Received: 30 January 2025
Revised: 20 February 2025
Accepted: 22 February 2025
Published: 25 February 2025

Citation: Kenzhaliyev, B.; Surkova, T.; Berkinbayeva, A.; Baltabekova, Z.; Smailov, K.; Abikak, Y.; Saulebekkyzy, S.; Tolegenova, N.; Omirbek, T.; Dosymbaeva, Z. Innovative Methods for Intensifying the Processing of Zinc Clinker: Synergy of Microwave Treatment and Ultrasonic Leaching. *Metals* **2025**, *15*, 246. <https://doi.org/10.3390/met15030246>

Copyright: © 2025 by the authors. Licensee MDPI, Basel, Switzerland. This article is an open access article distributed under the terms and conditions of the Creative Commons Attribution (CC BY) license (<https://creativecommons.org/licenses/by/4.0/>).

Keywords: zinc; clinker; microwave roasting; phase transformation; ultrasonic; leaching

1. Introduction

In recent decades, the significant depletion of high-grade ores has inevitably driven the search for and development of innovative methods to extract metals from unconventional raw material sources [1–5]. These sources include technogenic waste from polymetallic ores, dumps of substandard and off-grade ores, as well as resources from marine and oceanic deposits [6–10].

In industrially developed countries, the utilization rate of industrial waste reaches 70–80% [11,12]. For Kazakhstan, a major producer of mineral products with significant mining potential, the issue of industrial waste recycling holds particular importance [13–15]. The low utilization rate of technogenic raw materials in the country is primarily due to a lack of technologies and equipment for processing various types of waste [16]. Notably, the production cost of marketable products derived from industrial waste is generally lower than that of products obtained from traditionally mined ores. One of the key advantages of technogenic dumps is their readiness for processing, as the ores have already been extracted, washed, and disintegrated [17,18].

In the CIS countries, the annual volume of mined solid minerals is approximately 3.5 billion cubic meters. Including preparatory and beneficiation operations, this volume increases to around 5 billion cubic meters. Alongside this, approximately 1.5 billion cubic

meters of rock are mined annually, most of which, after beneficiation, is stockpiled in dumps and tailings storage facilities to enable the extraction of primary minerals from the Earth's crust [19].

Amid declining metal content in ores [20] and increasing volumes of refractory raw materials [21,22], transitioning to the comprehensive processing of low-grade, off-grade, and hard-to-reach mineral resources becomes both economically viable and scientifically justified [23]. Additionally, the use of technogenic raw materials as a secondary source of valuable elements is gaining relevance. Such materials are found in dumps and tailings storage facilities, which is particularly characteristic of countries like Kazakhstan, the USA, Finland, Poland, Canada, China, and South Africa. This approach significantly enhances the efficiency of mineral resource utilization while minimizing environmental impact and optimizing the economic performance of the mining and processing industries [24].

One of the most significant types of waste deserving particular attention is clinker, a technogenic byproduct of zinc production [25]. Clinker contains a variety of valuable compounds, including gold, silver, and copper. Of particular importance is the presence of zinc compounds, a highly valued non-ferrous metal widely used in the metallurgical industry [26]. The economic and technological feasibility of processing complex and refractory zinc-containing raw materials is driven by the possibility of extracting these valuable elements, which not only promotes the rational utilization of resources but also reduces the environmental burden through industrial waste recycling [27].

Currently, both pyrometallurgical [28] and hydrometallurgical [29,30] methods are employed to process zinc-containing technogenic raw materials. The most widely used pyrometallurgical technique is roasting, or reduction-distillation roasting, conducted at high temperatures of 1100–1300 °C with the addition of coke, constituting 35–45% of the processed material's mass [31]. This high-temperature process facilitates zinc evaporation and the formation of clinker enriched with valuable components, which are subsequently subjected to sulfuric acid leaching for further extraction. However, in Kazakhstan, an estimated 4.5 to 5.7 million tons of zinc industry waste has accumulated, underscoring the critical need for effective waste management and resource recovery strategies [32].

Traditional smelting processes are often associated with significant metal losses due to the volatility of zinc compounds and increased slag formation. The zinc recovery rate typically ranges from 70% to 85%, depending on furnace conditions and flux composition [33]. Despite the widespread application of pyrometallurgical processes, this method has notable disadvantages, including significant CO₂ emissions [34], high energy consumption, and the complexity of technological processes [35]. These shortcomings make it less suitable for processing high-silica zinc-containing technogenic raw materials due to the complex composition and structure of these materials' matrices. As a result, such raw materials often remain unprocessed and stored in sludge fields and tailings facilities, leading to substantial environmental and economic challenges [36].

Given the pressing issues surrounding the processing of refractory zinc-containing raw materials, the development of innovative and highly efficient technologies has become imperative. Currently, promising research directions include the application of microwave irradiation and ultrasonic treatment as preliminary processing stages.

Microwave irradiation, due to its mechanism of selective dielectric heating [26,37,38], induces localized thermal gradients and microstructural disruptions. This significantly enhances the reactivity and extractability of target elements [39]. Empirical studies have demonstrated that microwave treatment substantially improves the kinetics of leaching and extraction processes. Microcracks and mineral phase transformations in the matrix improve the penetration of leaching reagents, leading to more efficient metal recovery.

This approach also conserves energy, as targeted heating reduces the overall energy input required for subsequent processing stages [40,41].

Ultrasonic methods, driven by cavitation effects [42,43], play a pivotal role in enhancing the efficiency of metal leaching from ores and industrial waste [44]. Cavitation induced by ultrasound improves reagent transport, increases contact surface area, and promotes the penetration of leaching agents into the material, significantly intensifying metal extraction processes and reducing waste generation [45]. The interaction of ultrasonic waves with the treated medium leads to the dispersion of solid particles, the formation of microbubbles, and the generation of microjets, which reduce the thickness of the diffusion layer and accelerate dissolution reactions. The combination of ultrasonic treatment with oxidative leaching substantially enhances process kinetics while lowering activation energy [46–48].

The integration of ultrasonic technology with microwave irradiation represents an innovative approach that significantly improves the efficiency and transformation degree of materials during processing. These technologies profoundly influence the physicochemical properties of materials, creating favorable conditions for the intensification of chemical reactions and the optimization of process parameters. This integrated method facilitates the development of highly efficient and resource-saving technologies that align with modern requirements for environmental sustainability and the optimization of mineral and technogenic material processing. Such an approach offers promising prospects for the more complete extraction of metals from complex multicomponent systems, which is of critical importance for hydrometallurgy and related industries.

The aim of this study is to conduct a theoretical and experimental analysis of the synergistic effects of microwave treatment and ultrasonic cavitation on the kinetics of zinc clinker leaching in a sulfuric acid medium. Special attention is given to the detailed characterization of mass transfer mechanisms and phase transformations within the clinker matrix induced by the high-energy effects of localized cavitation collapse zones and selective dielectric heating. This comprehensive approach enables the clarification of the roles of passivation layer activation, agglomerate destruction, and the increase in reactive surface area in the kinetic patterns of leaching. The obtained results expand the fundamental understanding of the interaction between ultrasound and microwaves with multicomponent systems and provide a basis for the development of energy-efficient hydrometallurgical technologies for processing complex technogenic materials.

2. Materials and Methods

2.1. Materials

The subject of this study is refractory technogenic waste from zinc production in the form of clinker. Results of X-ray fluorescence analysis reveal that the clinker contains significant amounts of iron (37.53%), calcium (3.81%), silicon (4.58%), oxygen (41.64%), copper (1.04%), zinc (over 1.2%), and other elements, as detailed in Table 1.

Table 1. X-ray fluorescence analysis of the clinker (reprinted from Ref. [49]).

Elemental Content, %											
O	Na	Mg	Al	Si	P	S	Cl	K	Ca	Ti	Cr
41.644	0.173	1.030	0.912	4.581	0.055	0.807	0.011	0.109	3.807	0.101	0.020
Mn	Fe	Ni	Cu	Zn	As	Sr	Zr	Mo	Sb	Ba	Pb
0.110	37.532	0.033	1.037	1.217	0.138	0.043	0.012	0.026	0.034	0.825	0.154

The X-ray fluorescence (XRF) analysis of the clinker provides a quantitative assessment of its elemental composition, offering crucial insights into the chemical nature of the material. This compositional data is fundamental for selecting appropriate processing methods

and optimizing the extraction of valuable components. The results from the XRF analysis formed the basis for subsequent experimental investigations, focusing on the influence of microwave irradiation and ultrasonic treatment on structural and phase transformations. Particular emphasis was placed on evaluating reagent penetration within the clinker matrix and its impact on the leaching kinetics and efficiency of valuable metal recovery.

2.2. Analytical Techniques

This study utilizes advanced analytical techniques to investigate the phase composition of clinker and to elucidate the mechanisms of phase transformations. The phase composition of the samples was analyzed using a Bruker D8 Advance X-ray diffractometer (Bruker, Ettlingen, Germany) under the following conditions: 4–90° scan range, Cu-K α radiation ($\lambda = 0.15406$ nm), tube voltage of 40 kV, tube current of 40 mA, and a continuous scanning speed of 1°/min. Elemental composition was determined using an Axios 1 kW wavelength-dispersive X-ray fluorescence spectrometer (PANalytical, Almelo, the Netherlands), with data processing and interpretation performed using SuperQ5 software (Omnian 37). The surface microstructure was examined using a JXA-8230 electron probe microanalyzer (JEOL, Tokyo, Japan) operated at an accelerating voltage of 20 kV, an electron beam current below 1 nA, and aperture diaphragm No. 3. Energy-dispersive spectrometry (EDS) microanalysis (JEOL, Tokyo, Japan) was conducted with an electron beam current up to 6 nA and a dead time of up to 14%. Quantitative zinc concentrations in solutions and solid samples were measured using an Optima 8300DV inductively coupled plasma atomic emission spectrometer (PerkinElmer, Inc., Waltham, MA, USA) and an AA-7000 atomic absorption spectrometer (Shimadzu, Kyoto, Japan).

2.3. Experimental Method

The zinc leaching process from clinker consists of three key stages: grinding the clinker to achieve 90% of the fraction size below –0.071 mm, microwave phase transformation, and ultrasonic-assisted leaching. The technology involves several detailed steps, as shown in Figure 1. Initially, sample preparation is conducted, followed by roasting the clinker in a high-temperature microwave reactor of the “ENERGIA K-50” unit (Ust-Kamenogorsk, Kazakhstan) (915 MHz, 25 kW). This reactor is characterized by high power, operational stability, and enhanced efficiency [50,51]. Subsequently, the clinker undergoes leaching, as illustrated in Figure 2.

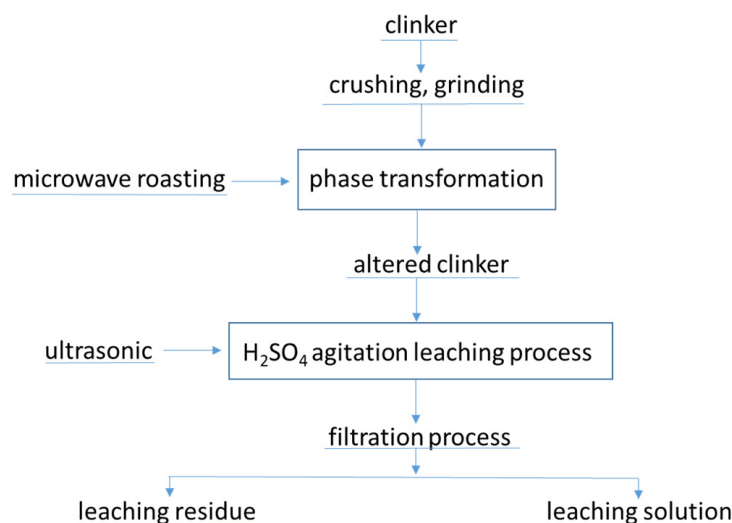


Figure 1. A flow diagram of the experiment.

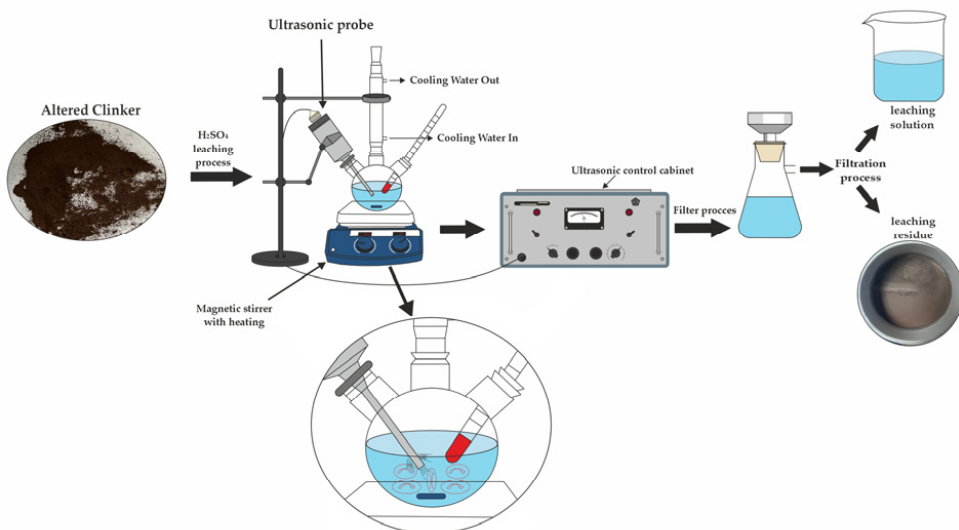


Figure 2. Schematic diagram of the leaching experimental setup. The lower part of the figure illustrates the ultrasonic probe and the cavitation effect, where microbubbles collapse, generating localized high pressure and temperature, which enhances the leaching efficiency.

For graph generation and data analysis during the experiment, Origin software (Origin Pro 9.8.0.200) was utilized. The zinc leaching rate was calculated using the following formula:

$$\eta_{Zn} = \left(\frac{(w_{clk.} \times m_{clk.}) - (w_{res} \times m_{res})}{w_{clk.} \times m_{clk.}} \right) \times 100\% \quad (1)$$

where η_{Zn} —zinc leaching rate (%); $w_{clk.}$ —zinc content in the initial clinker (%); w_{res} —zinc content in the residue after leaching (%); $m_{clk.}$ —mass of the initial clinker (g); and m_{res} —mass of the residue after leaching (g).

During the experiments, a controlled variable approach was applied to evaluate the effects of factors such as reaction temperature, sulfuric acid concentration, leaching duration, and pulp density. Four series of experiments were conducted under identical experimental conditions, as indicated by the asterisks in Table 2. To ensure the reliability of the results, each experiment was repeated at least three times, and the average values of the obtained data were used for analysis.

Table 2. Leaching parameters and ranges applied in the experiments.

Parameter	Value
Time (min)	30, 60 *, 120, 240, 300, 360
H ₂ SO ₄ Concentration (g/dm ³)	20, 40, 60, 80, 100 *, 120, 140, 160
Pulp Density (%)	20 *, 25, 35
Temperature (°C)	20, 40, 60 *, 80

* These parameters were kept constant.

2.4. Optimal Experimental Design for Leaching Process

To determine the optimal conditions and enhance the accuracy and reproducibility of the results, this study analyzed the zinc extraction process from clinker using the response surface methodology (RSM) and central composite design (CCD). The independent factors considered included temperature, sulfuric acid concentration, leaching duration, and pulp density (solid-to-liquid ratio). The application of the RSM mathematical approach enabled

the development of a second-order model describing the relationship between the response variable (zinc extraction) and the input parameters:

$$y = b_0 + \sum_{i=1}^k b_i x_i + \sum_{i=1}^k b_{ii} x_i^2 + \sum_{i=1}^{k-1} \sum_{j=i+1}^k b_{ij} x_i x_j \quad (2)$$

where y is the predicted zinc extraction value, b_0 is the constant coefficient, b_i represents the linear coefficients, b_{ii} denotes the quadratic coefficients, b_{ij} are the interaction coefficients between variables, and k is the number of factors.

The experiments were designed and analyzed using Design Expert 7.0 software (Stat-Ease, Inc., Minneapolis, MN, USA), which facilitated the development of a second-order regression model with high predictive accuracy.

The optimal levels and ranges of the variables—temperature, sulfuric acid concentration, leaching duration, and pulp density—identified as independent factors are presented in Table 3.

Table 3. Levels and codes of factors for CCD.

Factors	Symbol	Coding Level		
		-1	0	1
Time (min)	A	30	195	360
H ₂ SO ₄ Concentration (g/dm ³)	B	20	90	160
Pulp Density (%)	C	20	25	35
Temperature (°C)	D	20	50	80

3. Results and Discussion

3.1. Mineralogical Characteristics of the Clinker

Mineralogical analysis of the clinker was performed using an OLYMPUS BX51 microscope (Olympus Corporation, Tokyo, Japan). The typical structure and particle size of the minerals comprising the clinker are presented in Figure 3. The mineralogical examination revealed the presence of several key minerals, including sphalerite (ZnS), which appears as rare, fine-grained anhedral particles, chalcopyrite (CuFeS₂), commonly associated with pyrite (FeS₂) and sphalerite, as well as hematite (Fe₂O₃) and carbonaceous inclusions of varying sizes and shapes.

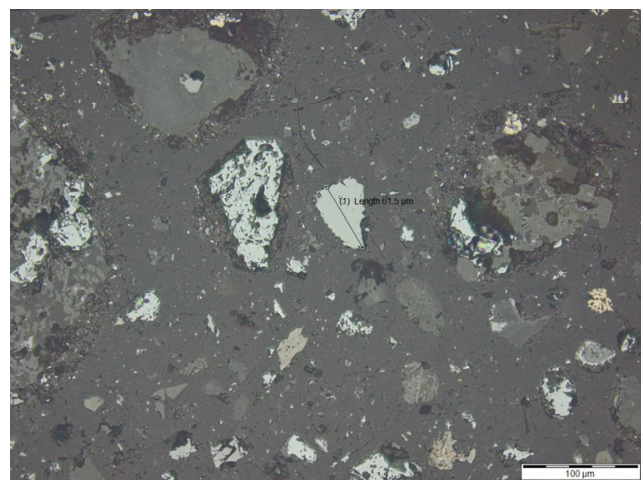


Figure 3. Sphalerite.

X-ray phase analysis identified hematite (24.2%) and magnesium iron oxide (18.2%) as the primary phase components of the clinker. Additional phase components are presented in Figure 4 and Table 4.

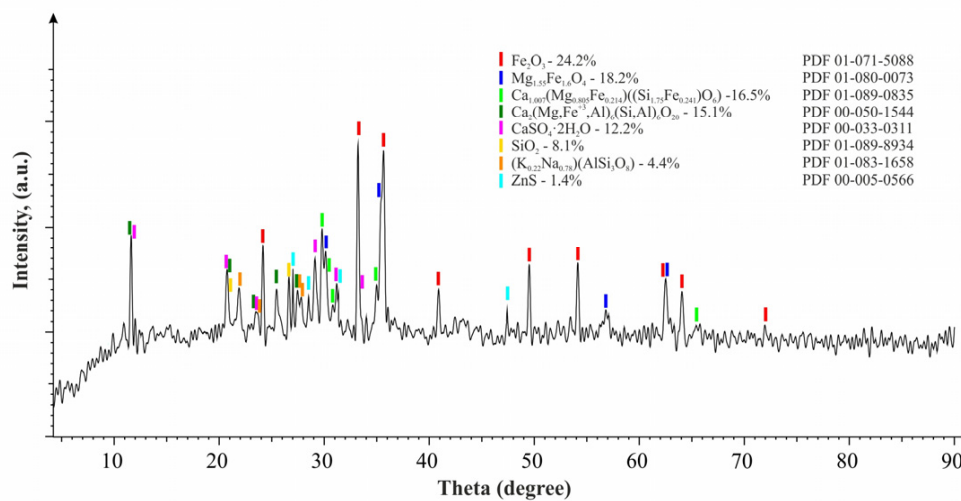


Figure 4. Diffractogram of the clinker (reprinted from Ref. [49]).

Table 4. Results of the X-ray phase analysis of the clinker (reprinted from Ref. [49]).

Compound Name	Formula	S-Q, %
Hematite	Fe_2O_3	24.2%
Magnesium iron oxide	$\text{Mg}_{1.55}\text{Fe}_{1.04}\text{O}_4$	18.2%
Diopside, ferrian	$\text{Ca}_{1.007}(\text{Mg}_{0.805}\text{Fe}_{0.214})_6(\text{Si}_{1.75}\text{Fe}_{0.241})\text{O}_6$	16.5%
Calcium magnesium iron aluminum silicate	$\text{Ca}_2(\text{Mg},\text{Fe}^{+3},\text{Al})_6(\text{Si},\text{Al})_6\text{O}_{20}$	15.1%
Gypsum	$\text{CaSO}_4 \cdot 2\text{H}_2\text{O}$	12.2%
Quartz	SiO_2	8.1%
Albite, potassian	$(\text{K}_{0.22}\text{Na}_{0.78})(\text{AlSi}_3\text{O}_8)$	4.4%
Sphalerite	ZnS	1.4%

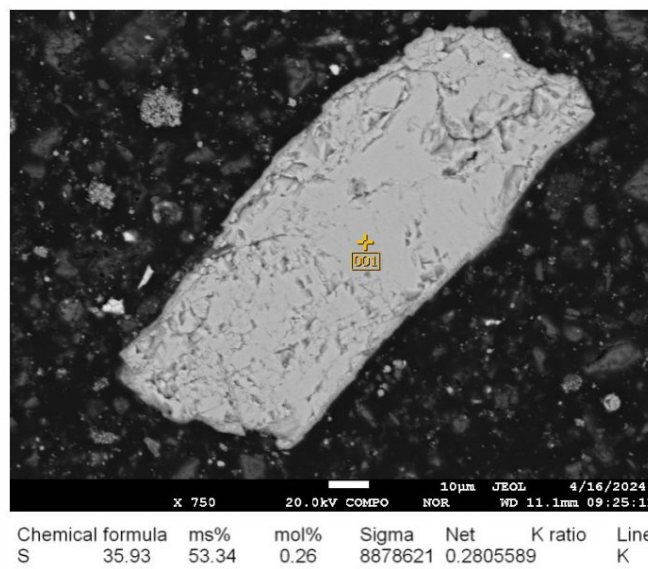
3.2. Phase Transformation via Microwave Irradiation

Based on the data from our previous study [49], which extensively investigated the phase changes in clinker at various temperatures, the optimal conditions for microwave roasting were determined to be 600 °C for 5–7 min. Under these conditions, the best conversion of zinc-containing phases into zinc oxide (ZnO) is achieved, according to the following chemical reaction:

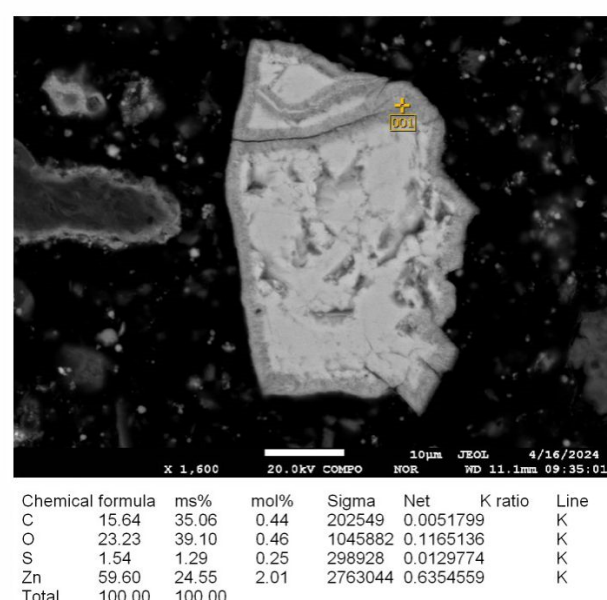


In this study, these conditions were applied to clinker treatment. Microwave roasting at 600 °C for 5–7 min effectively transforms sphalerite into zinc oxide (Figure 5).

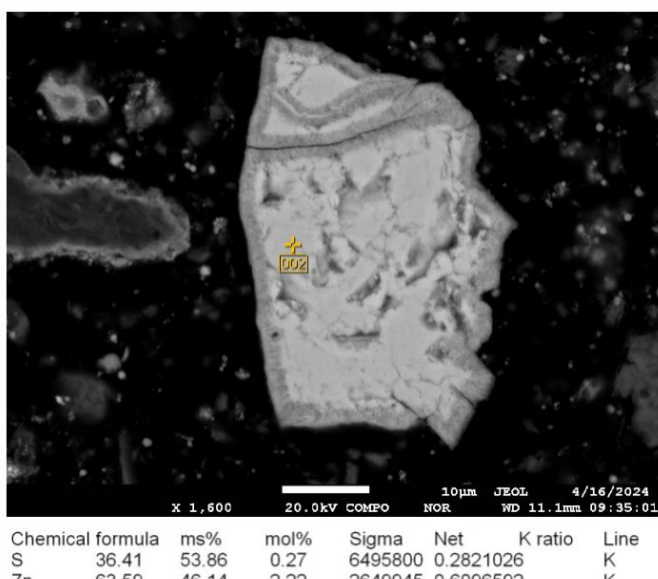
The microwave roasting process induces significant changes in the composition and microstructure of sphalerite. In its initial state, prior to microwave irradiation (Figure 5a), sphalerite is characterized by a high sulfur content (35.93%) and zinc content (64.07%). After irradiation at 600 °C for 3–4 min (Figure 5b), the sulfur content on the external surface significantly decreases to 1.54%, while the zinc content is reduced to 59.60%. Concurrently, oxygen appears (23.23%), indicating the onset of oxidative reactions on the mineral's surface and partial conversion of sphalerite to zinc oxide. However, analysis of the internal region of the same sample (Figure 5c) reveals a higher sulfur content (36.41%) and zinc content (63.59%), similar to the initial state (Figure 5a), suggesting incomplete material conversion.



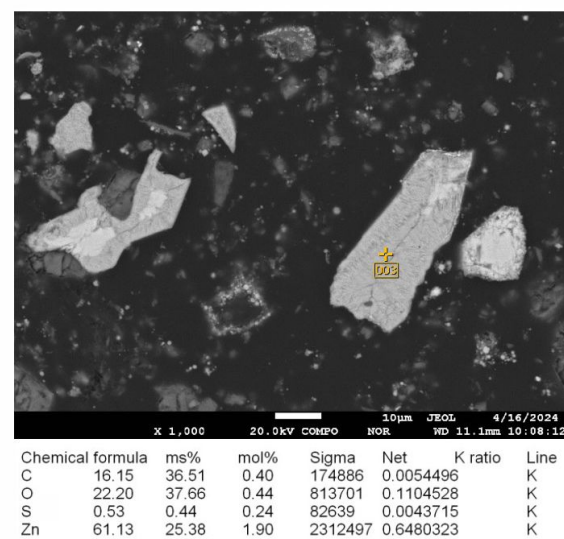
(a)



(b)



(c)



(d)

Figure 5. (a) Microstructure of the initial sample and energy-dispersive analysis of sphalerite prior to microwave irradiation at 25 °C; (b,c) microstructure and energy-dispersive analysis of sphalerite after microwave irradiation at 600 °C for 3–4 min; (d) microstructure and energy-dispersive analysis of sphalerite after microwave irradiation at 600 °C for 5–7 min.

A sample exposed to irradiation at 600 °C for 5–7 min (Figure 5d) demonstrates nearly complete transformation of sphalerite into zinc oxide, as evidenced by the presence of oxygen (22.20%). The sulfur content decreases to 0.53%, while the zinc content reaches 61.13%. These results confirm that the optimal microwave roasting conditions of 5–7 min ensure a high degree of sphalerite conversion to zinc oxide, which is a key factor for efficient material processing.

The detection of carbon in the samples is attributed to its deposition under the electron beam during microprobe analysis. The source of the carbon is the carbon tape used as a binding material during sample preparation for microprobe analysis.

3.3. Statistical Analysis and Model Fitting

3.3.1. Data Analysis

Table 5 displays the results of the analysis of variance (ANOVA) for the response surface model of the zinc leaching process from clinker.

Table 5. ANOVA for response surface quadratic model.

Source	Sum of Squares	df	Mean Square	F Value	p-Value Prob > F	Standard Error	95% CI (Lower–Upper)
Model	5466.47	14	390.46	4.39	0.0037	-	-
D- temperature	497.65	1	497.65	5.59	0.0319	±12.4	(470.2–525.1)
AD Interaction	1122.80	1	1122.80	12.62	0.0029	±18.7	(1085.5–1160.3)
BD Interaction	460.63	1	460.63	5.18	0.0380	±10.5	(438.2–483.1)
CD Interaction	414.24	1	414.24	4.65	0.0476	±9.8	(395.1–432.6)
A ² —Quadratic	1389.91	1	1389.91	15.62	0.0013	±22.5	(1350.4–1429.2)
D ² —Quadratic	346.96	1	346.96	3.90	0.0670	±8.6	(330.1–364.2)
Residual Error	1334.90	15	88.99	-	-	-	-
Lack of Fit	1290.90	10	129.09		0.1661		
Pure Error	44.00	5	8.80	-	-	-	-
Cor Total	6801.37	29	390.46	-	-	-	-

The F-statistic in analysis of variance (ANOVA) serves as a statistically grounded indicator of the proportion of variance explained by the model relative to the total variance. In this study, the F-statistic of the model, equal to 4.39, confirms its statistical significance according to the ANOVA results. The probability that such a high F-value could arise purely due to random factors is less than 0.1%, highlighting the reliability of the model.

The *p*-value of less than 0.0001 for the quadratic model further emphasizes its statistical significance. It is important to note that *p*-values not exceeding 0.05 are interpreted as confirming the significance of the corresponding factors. In this context, the significant components of the model include D, A, AD, and BD. To enhance the interpretation of the effects of significant factors, the model can be simplified to a regression equation focusing on the most significant variables with a 95% confidence level. The resulting regression equation is as follows:

$$\begin{aligned} E(Zn) = & -3.36 - 4.38A - 6.48B - 25.70C + 144.50D + 2.80AB - 36.32AC - \\ & 33.49AD + 18.19BC + 39.53BD + 170.46CD - 28.22A^2 - 1.65B^2 + 42.43C^2 \\ & + 20.32D^2 \end{aligned} \quad (4)$$

To improve the accuracy of assessing the adequacy of the quadratic model in approximating experimental data, several key diagnostic plots were developed and analyzed. Most experimental points are distributed along the diagonal axis, as shown in Figure 6a, indicating minimal deviations and high data reliability. The model errors demonstrate a normal distribution, as confirmed by the linear pattern of residual distribution. Further analysis of the random distribution of points along the t-axis (ranging from −3.00 to 3.00) and their proximity to zero, as seen in Figure 6b,c, supports the conclusion that the quadratic model effectively describes the relationship between the main experimental parameters and the leaching rate. This result underscores the reliability of the model and its suitability for predictive purposes.

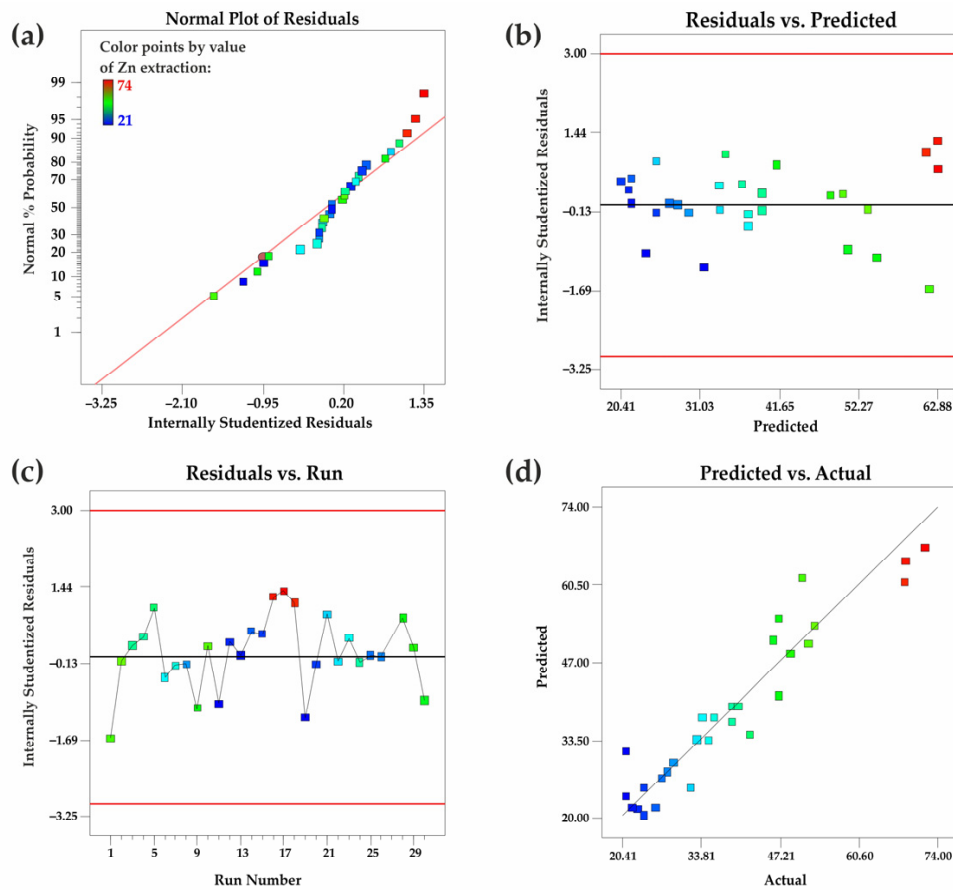


Figure 6. (a) A plot of normal probability vs. the internally studentized residuals, (b) internally studentized residuals vs. the predicted responses, (c) internally studentized residuals vs. run number, and (d) predicted responses vs. the actual values.

Figure 6d presents a diagram illustrating the relationship between predicted and actual values. The plot shows that the slope of the regression line approaches unity, with most points aligning along a straight line. This indicates a high degree of agreement between the calculated and experimental data, confirming the reliability and accuracy of the proposed quadratic model in predicting process parameters.

The analysis of the effects of experimental factors on zinc extraction efficiency (A: leaching duration; B: sulfuric acid concentration; C: pulp density; and D: temperature), as shown in Figure 7, reveals key trends. Temperature, sulfuric acid concentration, pulp density, and leaching duration exert significant influence on the zinc leaching rate from clinker.

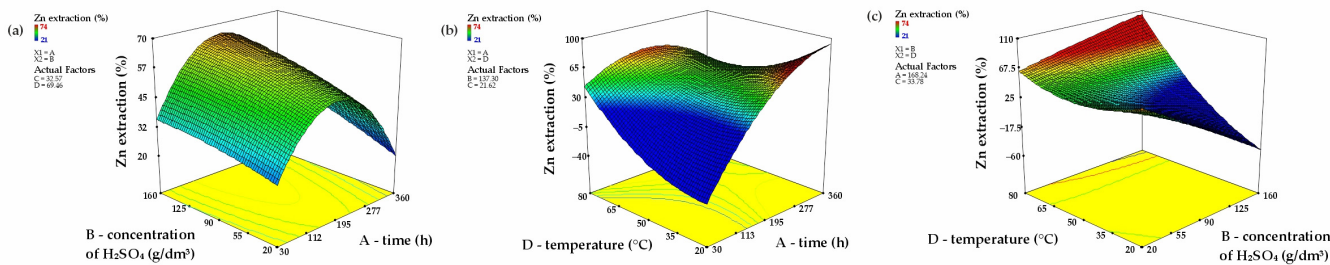


Figure 7. Three-dimensional response surfaces (with other parameters maintained at their central levels), illustrating the combined effects of B and A (a); D and A (b); D and B (c) (A—leaching duration, B—sulfuric acid concentration, D—temperature).

3.3.2. Internal Relationships Between Factors

The coefficients for factors A, B, C, and D are -4.38 , -6.48 , -25.70 , and $+144.50$, respectively, as presented in Equation (4). These values quantitatively reflect the impact of each factor on the target response, consistent with theoretical assumptions [52,53]. Analysis of the coefficients indicates that, except for temperature, all other investigated parameters have a negative influence on the zinc leaching rate.

Additionally, the order of the factors' influence on the leaching rate is as follows: temperature (D) > leaching duration (A) > sulfuric acid concentration (B) > pulp density (C).

The three-dimensional response surfaces, derived from the quadratic model, provide a comprehensive analysis of the interrelationship between key process factors and zinc extraction efficiency. Figure 7a examines the interaction between leaching duration (A) and sulfuric acid concentration (B). The analysis reveals that increasing both parameters significantly enhances zinc extraction. However, at high H_2SO_4 concentrations, a saturation point is reached, resulting in response stabilization. Contour plots confirm the dominant role of leaching duration, particularly in the initial stages of the reaction, highlighting its substantial contribution to the process kinetics.

Figure 7b illustrates the interaction between leaching duration (A) and temperature (D). The three-dimensional response surface graphs clearly indicate the predominant effect of temperature. As the temperature increases, the steepness of the surface rises significantly, particularly at longer leaching durations. Even at relatively short time intervals, high temperatures considerably accelerate the process, confirming its critical role in achieving maximum extraction efficiency.

Figure 7c presents the analysis of the interaction between sulfuric acid concentration (B) and temperature (D). The response surface plots demonstrate a synergistic effect between these factors: their simultaneous increase leads to a notable improvement in zinc extraction. Temperature retains its dominant importance, as evidenced by the steeper gradient of the surface along the temperature axis.

The results unequivocally underscore the pivotal role of temperature (D) as the primary factor determining process efficiency. It is followed by the interaction of leaching duration (A) and sulfuric acid concentration (B). Based on the analysis of F-values and factor interactions, the hierarchy of influence is as follows: AD > AC > BD > AB.

Each interaction factor has its own points of extreme values, enabling the prediction of optimal process conditions, as shown in Figure 7. The Design Expert 7.0 software was used for modeling and optimizing the zinc leaching process. According to the calculations, the optimal parameters included a sulfuric acid concentration of 140 g/dm^3 , pulp density of 20%, leaching duration of 2 h, and temperature of 80°C . Under these conditions, the predicted zinc extraction rate was 74.0%, with a desirability level of 0.967 for the model.

Experimental validation conducted under the optimized conditions confirmed the high accuracy of the model: the actual zinc extraction rate was 72.6%, which is close to the predicted value. This agreement demonstrates the reliability and predictive capability of the response surface-based model.

3.4. Effect of Ultrasonic-Assisted Leaching of Clinker

The phenomenon of ultrasonic cavitation and its impact on the leaching process are vividly illustrated in Figure 8. Cavitation induced by ultrasonic waves generates high-pressure microjets and shock waves, causing mineral particles to move turbulently and subjecting them to intense multidirectional impact forces. This dynamic environment plays a crucial role in enhancing the efficiency of zinc leaching [51].

Ultrasound was generated using a device (UZDN-LUCH 2, Almaty, Kazakhstan) operating at 15 kHz and 200 W, which ensured the stable formation of cavitation zones.

Ultrasonic cavitation significantly reduces diffusion resistance by creating a highly active interaction zone between the leaching solution and the mineral surface [54]. The collapse of cavitation bubbles produces localized high temperatures (up to 5000 K) and pressures (up to 1000 atm), effectively removing passivation layers from particle surfaces [55]. This exposes fresh, reactive surfaces, allowing sulfuric acid to interact more effectively with zinc-containing minerals. Furthermore, the mechanical action of microjets facilitates the disintegration of agglomerated particles, further increasing the reactive surface area.

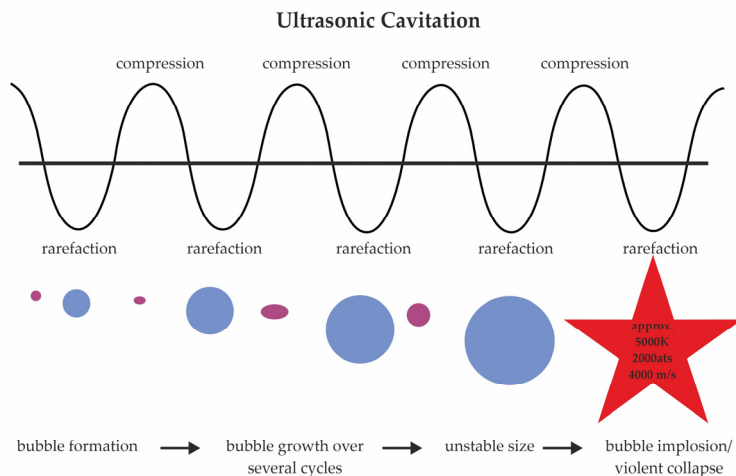


Figure 8. Ultrasonic cavitation.

The preliminary treatment of clinker using microwave irradiation, combined with leaching studies supported by mathematical modeling, enabled the determination of optimal conditions under which zinc recovery reached 72.6%. To further enhance efficiency, ultrasound was integrated into the leaching process. Figure 9 presents the results, demonstrating that the application of ultrasonic treatment increased zinc recovery by 4.1%, reaching 76.5%, compared to 72.6% achieved under identical conditions without ultrasound.

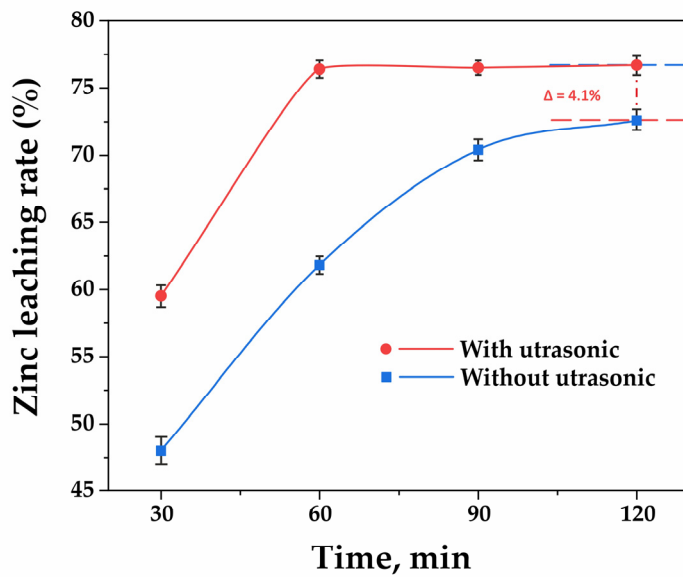


Figure 9. The effect of ultrasound on clinker leaching.

Experimental results demonstrated that applying ultrasonic treatment during leaching increased zinc recovery to 76.5% within just 1 h, compared to 72.6% achieved in 2 h without

ultrasound. This highlights the ability of ultrasound not only to enhance recovery but also to significantly reduce leaching time [56], showcasing the high efficiency of the technology.

4. Conclusions

This study demonstrates the effectiveness of a combined approach involving microwave thermal treatment and ultrasonic-assisted leaching to enhance zinc recovery from refractory clinker. The experimental results enabled the optimization of key leaching parameters, including sulfuric acid concentration, temperature, pulp density, and leaching time, while also assessing the influence of microwave treatment and ultrasonic cavitation on the dissolution rate.

Statistical data processing using response surface methodology (RSM) and central composite design (CCD) allowed for the identification of key trends in the effects of process parameters. It was shown that temperature plays a critical role in leaching efficiency, while the interaction between microwave treatment and ultrasonic cavitation enhances zinc recovery. Although the model demonstrated reasonable predictive capability within the experimental dataset, further research with an expanded data set is required to improve its accuracy and validate its applicability in industrial conditions.

Microwave treatment facilitated phase transformations that improved zinc solubility, whereas ultrasonic cavitation disrupted passivating layers and intensified mass transfer, resulting in enhanced leaching efficiency and reduced process duration. Under optimized conditions, zinc recovery reached 76.5%, confirming the potential of this approach for the hydrometallurgical processing of refractory materials.

Future research should focus on evaluating the economic feasibility of this method under industrial conditions, analyzing energy efficiency, and exploring alternative solvent systems to further enhance zinc recovery. Additionally, comparative studies with conventional leaching approaches and advanced process simulations could provide deeper insights into the scalability of this technique.

Author Contributions: Conceptualization, B.K., Z.B. and Y.A.; methodology, A.B., T.S., K.S. and S.S.; software, B.K., T.S., K.S. and N.T.; validation, B.K., A.B. and Y.A.; formal analysis, A.B. and N.T.; investigation, A.B., B.K. and Z.D.; resources, B.K., K.S. and T.O.; data curation, Z.B., A.B. and T.O.; writing—original draft preparation, Z.B. and S.S.; writing—review and editing, Z.B., B.K., A.B. and Z.D.; visualization, T.S. and N.T.; supervision, Z.B. and Y.A.; project administration, B.K., Z.B. and S.S.; funding acquisition, B.K. and Z.B. All authors have read and agreed to the published version of the manuscript.

Funding: This research is funded by the Science Committee of the Ministry of Science and Higher Education of the Republic of Kazakhstan (Grant No. AR 19675985).

Institutional Review Board Statement: Not applicable.

Informed Consent Statement: Not applicable.

Data Availability Statement: The original contributions presented in this study are included in the article. Further inquiries can be directed to the corresponding authors.

Conflicts of Interest: The authors declare no conflict of interest.

Abbreviations

The following abbreviations are used in this manuscript:

MDPI	Multidisciplinary Digital Publishing Institute
DOAJ	Directory of open access journals
TLA	Three letter acronym
LD	Linear dichroism

References

- Sharipova, A.S.; Linnik, K.A.; Zagorodnyaya, A.N.; Bakhytuly, N. Behaviour of lead and selenium during sequential sodium carbonate and nitric acid leaching of slime generated by the sulphuric acid plant of the Balkhash copper smelter. *Tsvetnye Met.* **2021**, *35*–42. [[CrossRef](#)]
- Ultarakova, A.A.; Yessengaziyev, A.M.; Kuldeyev, E.I.; Kassymzhanov, K.K.; Uldakhanov, O.K. Processing of Titanium Production Sludge with the Extraction of Titanium Dioxide. *Metalurgija* **2021**, *60*, 411–414.
- Panichkin, A.; Kenzhegulov, A.; Mamaeva, A.; Uskenbayeva, A.; Kshibekova, B.; Imbarova, A.; Alibekov, Z. Effect of Carbon and Cooling Rate on the Structure of Hypereutectic High Chromium Cast Iron in the Cast State and after Heat Treatment. *J. Compos. Sci.* **2023**, *7*, 483. [[CrossRef](#)]
- Ospanov, K.; Smailov, K.; Nuruly, Y. Patterns of Non-Traditional Thermodynamic Functions $\Delta rG_0/n$ and ΔfG_0 (Averaged) Changes for Cobalt Minerals. *Chem. Bull. Kazakh Natl. Univ.* **2020**, *96*, 22–30. [[CrossRef](#)]
- Kenzhaliyev, B.K.; Tussupbayev, N.K.; Abdykirova, G.Z.; Koizhanova, A.K.; Fischer, D.Y.; Baltabekova, Z.A.; Samenova, N.O. Evaluation of the Efficiency of Using an Oxidizer in the Leaching Process of Gold-Containing Concentrate. *Processes* **2024**, *12*, 973. [[CrossRef](#)]
- Ju, J.; Feng, Y.; Li, H.; Ma, R.; Li, Y.; Zhao, H.; Wang, H.; Jiang, S. An Innovative Method for the Efficient and Selective Extraction of Co, Ni, Cu, and Mn from Oceanic Cobalt-Rich Crusts by Ammonium Sulfate Roasting: Behavior, Roasting Kinetics and Mechanism. *Miner. Eng.* **2024**, *207*, 108543. [[CrossRef](#)]
- Zhao, F.; Jiang, X.; Wang, S.; Feng, L.; Li, D. The Recovery of Valuable Metals from Ocean Polymetallic Nodules Using Solid-State Metalized Reduction Technology. *Minerals* **2019**, *10*, 20. [[CrossRef](#)]
- Sakellariadou, F.; González, F.J.; Hein, J.R.; Rincón-Tomás, B.; Arvanitidis, N.; Kuhn, T. Seabed Mining and Blue Growth: Exploring the Potential of Marine Mineral Deposits as a Sustainable Source of Rare Earth Elements (MaREEs) (IUPAC Technical Report). *Pure Appl. Chem.* **2022**, *94*, 329–351. [[CrossRef](#)]
- Wegerer, S.; Semel, M.D.; Weixler, L. Vertical Exploration Approach for Seafloor Massive Sulfide Deposits. In Proceedings of the Offshore Technology Conference, Houston, TX, USA, 1–4 May 2023; ISBN 978-1-61399-974-5. [[CrossRef](#)]
- Balaram, V. Deep-Sea Mineral Deposits as a Future Source of Critical Metals, and Environmental Issues—A Brief Review. *Miner. Miner. Mater.* **2023**, *2*, 5. [[CrossRef](#)]
- Nath, S.; Singh, K.K.; Tangjang, S.; Das, S. Industrial Solid Wastes and Environment: An Overview on Global Generation, Implications, and Available Management Options. In *Springer Water*; Springer: Berlin/Heidelberg, Germany, 2024; pp. 221–246. [[CrossRef](#)]
- Varjani, S. Trends in Mitigation of Industrial Waste: Global Health Hazards, Environmental Implications and Waste Derived Economy for Environmental Sustainability. *Sci. Total Environ.* **2022**, *811*, 152357. [[CrossRef](#)]
- Bazarbayeva, S.M. Dataset on Industrial Waste Compositions in West Kazakhstan and Conditions for Processing Them into Construction Materials. *Data Brief* **2024**, *54*, 110265. [[CrossRef](#)] [[PubMed](#)]
- Kenzhaliyev, B.; Surkova, T.; Berkinbayeva, A.; Amanzholova, L.; Mishra, B.; Abdikerim, B.; Yessimova, D. Modification of Natural Minerals with Technogenic Raw Materials. *Metals* **2022**, *12*, 1907. [[CrossRef](#)]
- Dosmukhamedov, N.; Zholdasbay, E.; Argyn, A. Integrated Chlorination Technology for Producing Alumina and Silica from Ash-Slag Waste of the TPP of Kazakhstan. *J. Mater. Res. Technol.* **2022**, *23*, 1435–1446. [[CrossRef](#)]
- Zhanikulov, N.N.; Sapargaliyeva, B.; Agabekova, A.B.; Alfereva, Y.O.; Syrlybekkyzy, S.; Nurshakhanova, L.K.; Nurbayeva, F.K.; Sabyrbaeva, G.S.; Kozlov, P.T.; Kolesnikova, O.G. Studies of Utilization of Technogenic Raw Materials in the Synthesis of Cement Clinker from It and Further Production of Portland Cement. *J. Compos. Sci.* **2023**, *7*, 226. [[CrossRef](#)]
- Jandieri, G. Increasing the Efficiency of Secondary Resources in the Mining and Metallurgical Industry. *J. S. Afr. Inst. Min. Metall.* **2023**, *123*, 1–8. [[CrossRef](#)]
- Krishnan, S.; Zulkapli, N.S.; Kamyab, H.; Taib, S.M.; Din, M.F.M.; Majid, Z.A.; Chaiprapat, S.; Kenzo, I.; Ichikawa, Y.; Nasrullah, M.; et al. Current Technologies for Recovery of Metals from Industrial Wastes: An Overview. *Environ. Technol. Innov.* **2021**, *22*, 101525. [[CrossRef](#)]
- Kolesnikov, A.; Fediuk, R.; Kolesnikova, O.; Zhanikulov, N.; Zhakipbayev, B.; Kuraev, R.; Akhmetova, E.; Shal, A. Processing of Waste from Enrichment with the Production of Cement Clinker and the Extraction of Zinc. *Materials* **2022**, *15*, 324. [[CrossRef](#)]
- Rahmati, S.; Adavodi, R.; Hosseini, M.R.; Veglio', F. Efficient Metal Extraction from Dilute Solutions: A Review of Novel Selective Separation Methods and Their Applications. *Metals* **2024**, *14*, 605. [[CrossRef](#)]
- Ultarakova, A.; Karshyga, Z.; Lokhova, N.; Yessengaziyev, A.; Kassymzhanov, K.; Mukangaliyeva, A. Studies of Niobium Sorption from Chloride Solutions with the Use of Anion-Exchange Resins. *Processes* **2023**, *11*, 1288. [[CrossRef](#)]
- Ultarakova, A.; Karshyga, Z.; Lokhova, N.; Yessengaziyev, A.; Kassymzhanov, K.; Mukangaliyeva, A. Studies on the Processing of Fine Dusts from the Electric Smelting of Ilmenite Concentrates to Obtain Titanium Dioxide. *Materials* **2022**, *15*, 8314. [[CrossRef](#)]

23. Abdulvaliev, R.A.; Surkova, T.Y.; Baltabekova, Z.; Yessimova, D.M.; Stachowicz, M.; Smailov, K.M.; Dossymbayeva, Z.D.; Ainur, B. Effect of Amino Acids on the Extraction of Copper from Sub-Conditional Raw Materials. *Complex Use Miner. Resour.* **2024**, *335*, 50–58. [[CrossRef](#)]
24. Walke, S.; Mandake, M.B. Optimization of Chemical Engineering Processes in the Mining and Metal Industry: A Review. *J. Mines Met. Fuels* **2024**, *71*, 240–251. [[CrossRef](#)]
25. Kuandykova, A.; Taimasov, B.; Potapova, E.; Sarsenbaev, B.; Kolesnikov, A.; Begentayev, M.; Kuldeyev, E.; Dauletiyarov, M.; Zhanikulov, N.; Amiraliyev, B.; et al. Production of Composite Cement Clinker Based on Industrial Waste. *J. Compos. Sci.* **2024**, *8*, 257. [[CrossRef](#)]
26. Toshkodirova, R.E.; Abdurakhmonov, S. Processing of Clinker—Technogenic Waste of Zinc Production. *Univ. Tech. Sci.* **2020**, *11*, 78–81.
27. Trebukhov, S.; Volodin, V.; Nitsenko, A.; Burabaeva, N.; Ruzakhunova, G. Recovery of Zinc from the Concentrate of Domestic Waste Processing by Vacuum Distillation. *Metals* **2022**, *12*, 703. [[CrossRef](#)]
28. Lobanov, V.G.; Kolmachikhina, O.B.; Polygalov, S.E.; Khabibulina, R.E.; Sokolov, L.V. Features of the Presence of Precious Metals in the Zinc Production Clinker. *Russ. J. Non-Ferr. Met.* **2022**, *63*, 594–598. [[CrossRef](#)]
29. Kiprono, N.R.; Kawalec, A.; Klis, B.; Smolinski, T.; Rogowski, M.; Kalbarczyk, P.; Samczynski, Z.; Norenberg, M.; Ostachowicz, B.; Adamowska, M.; et al. Radiation Techniques for Tracking the Progress of the Hydrometallurgical Leaching Process: A Case Study of Mn and Zn. *Metals* **2024**, *14*, 744. [[CrossRef](#)]
30. Maltrana, V.; Morales, J. The Use of Acid Leaching to Recover Metals from Tailings: A Review. *Metals* **2023**, *13*, 1862. [[CrossRef](#)]
31. Wang, S.; Gao, F.; Li, B.; Liu, Y.; Deng, T.; Zhang, Y.; Chen, W. Clinkerization of Carbonatable Belite–Melilite Clinker Using Solid Waste at Low Temperature. *Constr. Build. Mater.* **2024**, *418*, 135357. [[CrossRef](#)]
32. Zhidbekkyzy, A.; Temerbulatova, Z.; Amangeldiyeva, B.; Sakhariyeva, A. Towards a Circular Economy: An Analysis of Kazakhstani Case. *J. Econ. Res. Bus. Adm.* **2023**, *143*, 16–32. [[CrossRef](#)]
33. Qiao, Y.; Wang, G. Recent Status of Production, Administration Policies, and Low-Carbon Technology Development of China’s Steel Industry. *Metals* **2024**, *14*, 480. [[CrossRef](#)]
34. Diaz, F.; Sommerfeld, M.; Hovestadt, G.; Latacz, D.; Friedrich, B. Lessons Learned from Attempts at Minimising CO₂ Emissions in Process Metallurgy—Pyrolysed Secondary Raw Materials, Bio-Coke, and Hydrogen as Alternative Reducing Agents. In Proceedings of the 12th International Conference of Molten Slags, Fluxes and Salts, Brisbane, Australia, 17–19 June 2024. [[CrossRef](#)]
35. Harvey, J.-P.; Courchesne, W.; Vo, M.D.; Oishi, K.; Robelin, C.; Mahue, U.; Leclerc, P.; Al-Haiek, A. Greener Reactants, Renewable Energies and Environmental Impact Mitigation Strategies in Pyrometallurgical Processes: A Review. *MRS Energy Sustain.* **2022**, *9*, 212–247. [[CrossRef](#)] [[PubMed](#)]
36. Hamidi, A.; Nazari, P.; Shakibania, S.; Rashchi, F. Microwave Irradiation for the Recovery Enhancement of Fly Ash Components: Thermodynamic and Kinetic Aspects. *Chem. Eng. Process.* **2023**, *191*, 109472. [[CrossRef](#)]
37. Lin, S.; Li, K.; Yang, Y.; Gao, L.; Omran, M.; Guo, S.; Chen, J.; Chen, G. Microwave-Assisted Method Investigation for the Selective and Enhanced Leaching of Manganese from Low-Grade Pyrolusite Using Pyrite as the Reducing Agent. *Chem. Eng. Process.* **2021**, *159*, 108209. [[CrossRef](#)]
38. Al-Harahsheh, M.; Kingman, S.W. Microwave-Assisted Leaching—A Review. *Hydrometallurgy* **2004**, *73*, 189–203. [[CrossRef](#)]
39. Stojković, M.; Ristić, M.; Đolić, M.; Perić Grujić, A.; Onjia, A. Recovery of Rare Earth Elements from Coal Fly and Bottom Ashes by Ultrasonic Roasting Followed by Microwave Leaching. *Metals* **2024**, *14*, 371. [[CrossRef](#)]
40. Fang, X.; Peng, Z.; Yin, T.; Rao, M.; Li, G. Microwave Treatment of Copper–Nickel Sulfide Ore for Promotion of Grinding and Flotation. *Metals* **2024**, *14*, 565. [[CrossRef](#)]
41. Ye, L.; Peng, Z.; Tian, R.; Tang, H.; Zhang, J.; Rao, M.; Li, G. A novel process for highly efficient separation of boron and iron from ludwigite ore based on low-temperature microwave roasting. *Powder Technol.* **2022**, *410*, 117848. [[CrossRef](#)]
42. Tao, F.; Zhao, G.; Chen, W.; Tao, D. 1/2 Order Subharmonic Waves of Two Cavitation Bubbles. *Ultrason. Sonoch.* **2024**, *110*, 107022. [[CrossRef](#)]
43. Moussatov, A.; Granger, C.; Dubus, B. Cone-Like Bubble Formation in Ultrasonic Cavitation Field. *Ultrason. Sonoch.* **2003**, *10*, 191–195. [[CrossRef](#)]
44. Li, H.; Hu, C.; He, X.; Wang, J.; Tian, S.; Zhu, X.; Mao, X. Mechanism and Kinetics Study of Vanadium Leaching from Landfilled Metallurgical Residues by Ultrasonic with Ozonation Enhancement in a Low-Acid Medium. *Ultrason. Sonoch.* **2024**, *109*, 106998. [[CrossRef](#)] [[PubMed](#)]
45. Liu, B.; Shi, C.; Huang, Y.; Han, G.; Sun, H.; Zhang, L. Intensifying Separation of Pb and Sn from Waste Pb-Sn Alloy by Ultrasound-Assisted Acid Leaching: Selective Dissolution and Sonochemistry Mechanism. *Ultrason. Sonoch.* **2024**, *102*, 106758. [[CrossRef](#)]
46. Zhu, R.; Wang, S.; Chen, Y.; Xiang, D.; Zhang, L.; Liu, J.; Ye, J. Ultrasound Enhanced In-Situ Chemical Oxidation for Leaching Ag from Zinc Leaching Residue and Response Surface Optimization. *Chem. Eng. J.* **2024**, *489*, 151243. [[CrossRef](#)]

47. Zhang, D.; Fu, L.; Liu, H.; Li, H.; Wang, S.; Zhang, M.; Zhu, M.; Zhang, L. High-Efficiency Leaching of Chalcopyrite by Ozone with Ultrasonic Promotion: Kinetics and Mechanism. *J. Mol. Liq.* **2024**, *401*, 124682. [[CrossRef](#)]
48. Liu, L.; Gan, M.; Fan, X.; Gao, Z.; Sun, Z.; Ji, Z.; Wei, J.; Ma, S. Mechanism of Ultrasonic Enhanced Acetic Acid Efficiently Leaching of Steel Slag and Synthesis of Calcium Carbonate Whiskers. *Sep. Purif. Technol.* **2024**, *339*, 126615. [[CrossRef](#)]
49. Kenzhaliyev, B.; Surkova, T.; Berkinbayeva, A.; Baltabekova, Z.; Smailov, K. Harnessing Microwave Technology for Enhanced Recovery of Zinc from Industrial Clinker. *Metals* **2024**, *14*, 699. [[CrossRef](#)]
50. Ma, A.; Zheng, X.; Gao, L.; Li, K.; Omran, M.; Chen, G. Enhanced Leaching of Zinc from Zinc-Containing Metallurgical Residues via Microwave Calcium Activation Pretreatment. *Metals* **2021**, *11*, 1922. [[CrossRef](#)]
51. Liu, J.; Li, S.; Zhang, L.; Yang, K. Application of the Microwave and Ultrasonic Combined Technique in the Extraction of Refractory Complex Zinc Ore. *Metals* **2023**, *13*, 356. [[CrossRef](#)]
52. Chen, H.; Wu, D.; Wang, Z. Investigation of the Leaching Kinetics of Zinc from Smithsonite in Ammonium Citrate Solution. *Metals* **2024**, *14*, 519. [[CrossRef](#)]
53. Tian, J.J.; Wu, D.D.; Li, S.Y.; Ma, W.H.; Wang, R.Z. Effect of process variables on leaching behavior and kinetics of silver element from waste photovoltaic modules. *Sep. Purif. Technol.* **2024**, *335*, 126062. [[CrossRef](#)]
54. Scruby, C.B.; Drain, L.E. *Laser Ultrasonics: Techniques and Applications*; Routledge: London, UK, 2019.
55. Vargas, S.A.; Delgado-Macuil, R.J.; Ruiz-Espinosa, H.; Rojas-López, M.; Amador-Espejo, G.G. High-intensity ultrasound pretreatment influence on whey protein isolate and its use on complex coacervation with kappa carrageenan: Evaluation of selected functional properties. *Ultrason. Sonoch.* **2021**, *70*, 105340. [[CrossRef](#)]
56. Slaczka, A.S. Effect of ultrasound on ammonium leaching of zinc from galmei ore. *Ultrasonics* **1986**, *24*, 53–55. [[CrossRef](#)]

Disclaimer/Publisher’s Note: The statements, opinions and data contained in all publications are solely those of the individual author(s) and contributor(s) and not of MDPI and/or the editor(s). MDPI and/or the editor(s) disclaim responsibility for any injury to people or property resulting from any ideas, methods, instructions or products referred to in the content.